Microsyst Technol (2005) 11: 958–964
DOI 10.1007/s00542-005-0505-9

TECHNICAL PAPER

Nohyu Kim

Real time thickness measurement of thin film for end-point detector (EPD) of 12-inch spin etcher using the white light interferometry

Received: 3 July 2003 / Accepted: 17 December 2003 / Published online: 16 August 2005
© Springer-Verlag 2005

Abstract A real time thickness measurement method based on the wide band white light interferometry for spin etcher is presented for the silicon-oxide and poly-silicon film deposited on 12-inch silicon wafer subject to a rotational vibration and chemical flow. Mathematical model for the vibration and chemical flow is described using a statistical method and analyzed to investigate their effects on the interference of reflected lights from the thin films. A white light interferometry system for the real time thickness measurement of thin films have been also developed to evaluate the performance of the method in experiment and determine the thickness of the films using signal processing techniques including curve-fitting and adaptive filtering. Experiments conducted for thin films ranging form 100 nm to 600 nm in thickness show that the method proposed in the paper is proved to be effective with a good accuracy of maximum 1.8% error.

1 Introduction

End-point detector (EPD) is thin film measurement equipment developed to control the amount of etching thickness and the remaining time to stop the etching process, which is very critical in semiconductor industry to assure the quality and performance of the production line of wafers. Traditional EPD system widely used in plasma etcher called as dry etcher, measures the film thickness of the wafer sitting still in plasma gas without any motion or any chemicals on the wafer. However, in the spin etcher shown in Fig. 1 the wafer is etched by chemicals while it rotates at a high speed, so that the productivity is very good because of its etching speed and low cost (Quirk and Serda 2001). Especially in case of 12-inch wafer production line, the etching speed increases even more comparing to 8-inch wafer and the etching area almost doubles, so that the monitoring technique like EPD is vital to quality control and assurance. In addition, the uniformity of thin films is very important because the etching speed changes much in the radial direction of the 12-inch wafer (Kim 1999; Maynard and Hershkowitz 1995).

End-point detector system for the spin etcher requires special capabilities very different from that for the plasma etcher in its functions, one of which is the real-time measurement to enable to monitor the remaining thickness of the thin film during etching process. The other one, which is more critical to measure the thin film thickness in the spin etcher, is the accuracy of measurement because the interference signal from the thin film would deteriorate due to the rotational motion of the wafer and fluid flow generated by the chemicals. Therefore it is necessary to know how the disturbances (vibration and chemical flow) affect the interference characteristics and the measurement accuracy of the film thickness.

In this paper a single layer model for EPD considering the vibration and chemical flow is proposed and the interference pattern of reflected lights from the model is described. A prototype interferometer with software program to measure the thin film thickness using mathematical model were developed and applied to thin films including silicon-oxide and poly-silicon to investigate its effectiveness and performance.

N. Kim
School of Mechatronic Engineering,
Korea University of Technology and Education,
307 Gajeon-Ri, Byung-chun, Chunan,
330-860, Korea
E-mail: nykim@kut.ac.kr
Tel.: +82-41-5601126
Fax: +82-41-5601253

2 Theory of white light interferometry

Electric field of a light propagating in the direction of propagation vector **k** at a position of vector **r** with a

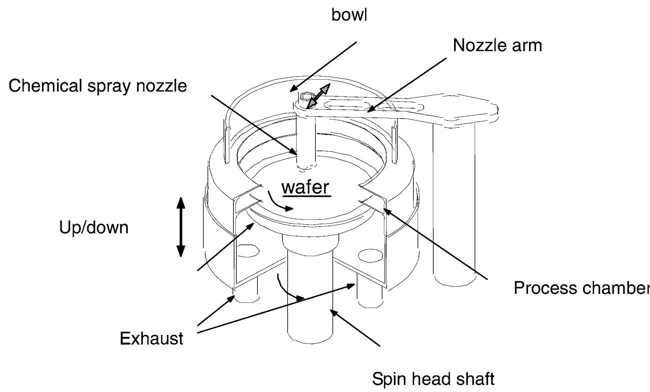

Fig. 1 Configuration of 12-inch wafer spin etcher

phase angle ϕ and amplitude E_0 is expressed by $E(t, \mathbf{r}) = E_0 \cdot \exp(i(\omega t + \mathbf{k} \cdot \mathbf{r} + \phi))$ and can be simplified in one-dimensional direction of x and in a medium of the refractive index n and the extinction coefficient κ as following (Xu et al. 1995)

$$E(t, x) = E_0 \cdot e^{-\kappa k x} \cdot e^{i(\omega t + nkx + \phi)}, \quad (1)$$

where k is the wave number of the light given by $2\pi/\lambda$ and λ is the wavelength of the light in the air. If the light is incident from the air of refractive index n to a transparent thin film deposited on the silicon substrate with the refractive index n_1 and the thickness h as shown in Fig. 2, two reflected lights, U_1 and U_2, are produced from the interfaces of the layered substrate. From the path difference of U_1 and U_2 in Fig. 2, the phase difference $\Delta\phi$ between U_1 and U_2 is calculated easily from the geometric condition if the difference of the path length is Δx, such as

$$\Delta\phi = k \cdot \Delta x = k \cdot \left(\frac{2n_1 h}{\cos\theta_1} - 2n_0 h \cdot \sin\theta_0 \tan\theta_1 \right) \quad (2)$$

In Eq. 2 the first term of the parenthesis represents the path difference inside the film and the second in the air. Even though additional phase changes of U_1 and U_2 take place during the reflection and transmission at the interfaces, it is neglected in this paper because its contribution is very small for the materials considered in the paper comparing to the path difference. The superposition of both U_1 and U_2 yields a constructive and destructive interference according to the phase difference, which leads to the variation of the intensity of the total reflected light measured in the optical probe. If the reflected lights, U_1 and U_2, are expressed in the form of Eq. 1 without the oscillating term $\omega\, t$, they becomes

$$U_1 = A_1 \cdot e^{i(nkx + \phi_1)} \text{ and } U_2 = A_2 \cdot e^{i(nkx + \phi_2)}, \quad (3)$$

where A_1 and A_2 are the amplitudes of the reflected lights U_1 and U_2, and ϕ_1 and ϕ_2 are the phase angle of lights, respectively. Then the intensity $\boldsymbol{I}$ of the total reflected light is given by (Wang et al. 1995)

$$\begin{aligned} \boldsymbol{I} &= \frac{1}{2Z}(U_1 + U_2) \cdot \overline{(U_1 + U_2)} \\ &= \boldsymbol{I}_1 + \boldsymbol{I}_2 + \frac{1}{2Z}(A_1 A_2 e^{i\Delta\phi} + A_1 A_2 e^{-i\Delta\phi}) \\ &= \boldsymbol{I}_1 + \boldsymbol{I}_2 + \frac{A_1 A_2}{2Z}\cos(\Delta\phi), \text{where } \Delta\phi = \phi_1 - \phi_2 \\ &= \boldsymbol{I}_1 + \boldsymbol{I}_2 + \frac{A_1 A_2}{2Z}\cos[(2kh)(n_1 \sec\theta_1 - n_0 \sin\theta_0 \tan\theta_1)] \end{aligned} \quad (4)$$

In Eq. 4 $\boldsymbol{I}_1$ and $\boldsymbol{I}_2$ are the intensities of U_1 and U_2 respectively and it gives the expression for the relationship between the thickness h of thin film and the intensity of total reflected light $\boldsymbol{I}$ over the range of wavelength (wave number) when using the white light. Interference pattern of SiO_2 simulated in the computer by Eq. 4 for the normal incidence is shown for example in Fig. 3.

However, in case that the wafer in the Fig. 2 rotates and vibrates, the light path and the incident angle θ_0 including refraction angles fluctuate with time due to the disturbance. Moreover the etching chemical flowing on the wafer with high speed may also affect the magnitude of reflected lights, A_1 and A_2, because of the attenuation of light energy in the chemical. This means that Eq. 4

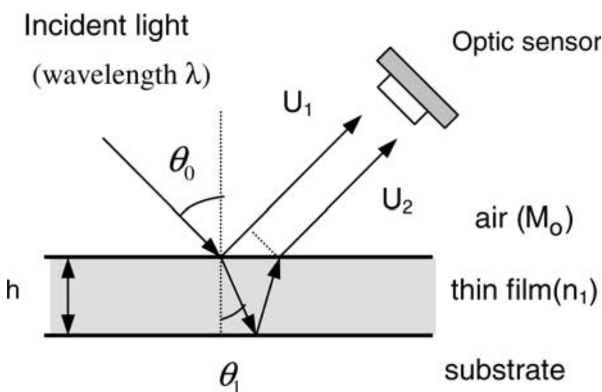

Fig. 2 Interference of reflected lights from a thin film

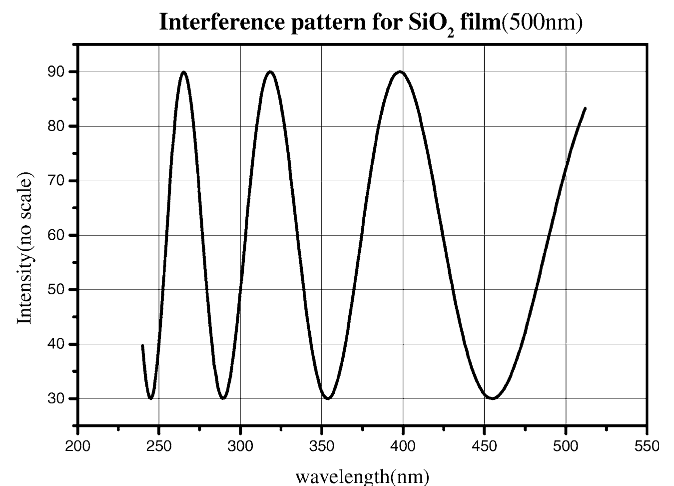

Fig. 3 Interference pattern of SiO_2 film(500 nm)

becomes corrupted and noisy due to the vibration and the chemical flow. In order to include the effects in Eq. 4, two random variables are introduced, which are the thickness d of the chemical and the incident angle ε_θ due to the vibration. Assuming that A_1 and A_2 are reduced only by the attenuation in the chemical of thickness d, the attenuated amplitudes of A_1 and A_2, $\hat{A}_1$ and $\hat{A}_2$, can be written using the extinction coefficient κ_c of the chemical by,

$$\begin{aligned}\hat{A}_1 &= A_1 e^{-\kappa_c kd} \approx A_1 \cdot (1 - \kappa_c kd),\\ \hat{A}_2 &= A_2 e^{-\kappa_c kd} \approx A_2 \cdot (1 - \kappa_c kd) \text{ for small } \kappa_c d\end{aligned} \tag{5}$$

It is also assumed that the incident angle θ_0 is a random variable with a mean value $\overline{\theta_0}$ and a random noise ε_θ, that is, $\theta_0 = \overline{\theta_0} + \varepsilon_\theta$. Accordingly the refraction angle is expressed as the random noise ε_θ from the Snell's law, which is $\theta_1 = n_0/n_1(\overline{\theta_0} + \varepsilon_\theta)$ for a small ε_θ. Then the total intensity $\boldsymbol{I}$ in Eq. 4 can be expressed for small d and normal incidence $(\overline{\theta_0}) = 0$ as

$$\begin{aligned}\boldsymbol{I}(k) &= (1 - k\cdot\kappa_c d)^2 \left\{ \boldsymbol{I}_1 + \boldsymbol{I}_2 + \frac{A_1A_2}{2Z}\cos[(2kh)(n_1\sec\theta_1 - n_0\sin\theta_0\tan\theta_1)] \right\}\\ &\approx (1 - 2k\cdot\kappa_c d)\left\{ \boldsymbol{I}_1 + \boldsymbol{I}_2 + \frac{A_1A_2}{2Z}\cos[2khn_1(1-\varepsilon_\theta^2)] \right\}\end{aligned} \tag{6}$$

Replacing the wave number k by ν for notational convenience, Eq. 6 becomes

$$\boldsymbol{I}(v) \approx (1 - 2v\cdot\kappa_c d)\left\{ \boldsymbol{I}_1 + \boldsymbol{I}_2 + \frac{A_1A_2}{2Z}\cos[2vhn_1(1-\varepsilon_\theta^2)] \right\} \tag{7}$$

In addition to the disturbances from the vibration and fluid flow, a random noise η_R due to the electrical noise and white noise from the environment corrupts the signal $\boldsymbol{I}$ as well, so that Eq. 7 is rewritten by

$$\begin{aligned}\boldsymbol{I}(v) \approx&(1 - 2v\cdot\kappa_c d)\\ &\left\{ \boldsymbol{I}_1 + \boldsymbol{I}_2 + \frac{A_1A_2}{2Z}\cos[2vhn_1(1-\varepsilon_\theta^2)] \right\} + \eta_R\\ &\approx (\boldsymbol{I}_1 + \boldsymbol{I}_2) + \frac{A_1A_2}{2Z}\cos(2vhn_1)\\ &\quad - (2v\cdot\kappa_c d)\left\{ \boldsymbol{I}_1 + \boldsymbol{I}_2 + \frac{A_1A_2}{2Z}\cos(2vhn_1) \right\}\\ &\quad + \frac{A_1A_2}{2Z}\sin(2vhn_1)\cdot\varepsilon_\theta^2 + \eta_R\end{aligned} \tag{8}$$

This equation indicates that the interference signal $\boldsymbol{I}$ in Eq. 4 is disturbed by the attenuation effect from the chemical thickness d, the vibration ε_θ, and the random white noise η_R. The first and second terms are the interference signal when there are no vibration and no chemical flow. The third term in Eq. 8 describes the interference signal induced by the chemical flow and the fourth one due to the vibration. It is clearly seen that the chemical effect can be much more severe than the vibration effect because it is directly coupled with the total mean intensity $\boldsymbol{I}_1 + \boldsymbol{I}_2$.

The intensity spectrum represented by Eq. 8 can be very different from the ideal interference pattern shown in Fig. 3 if $\kappa_c\, d$ of the chemical and vibration effect cannot be negligible. In Fig. 4, a distorted interference spectrum computed in the computer for an extreme case of $\kappa_c \cdot (d/h) = 0.1$ and $\varepsilon_\theta = 0$ is shown to describe the effect of chemical film on the spectrum signal, where the more distortion is made for the light of a shorter wavelength. The vibration effect on the spectrum of Eq. 8 is expected to act like a random noise such as η_R.

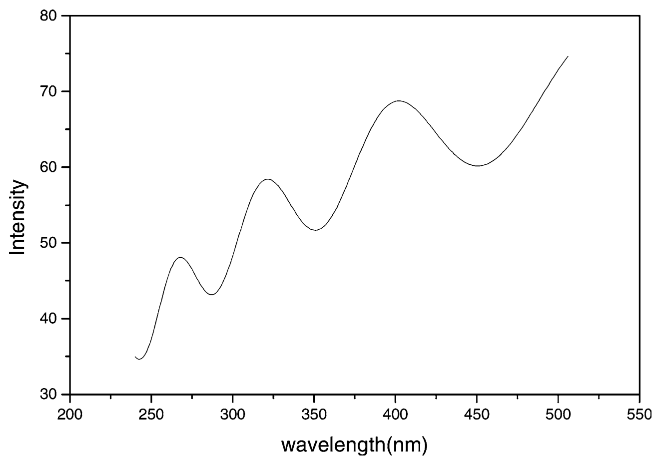

Fig. 4 Distortion of interference pattern from SiO_2 film due to a thick chemical flow

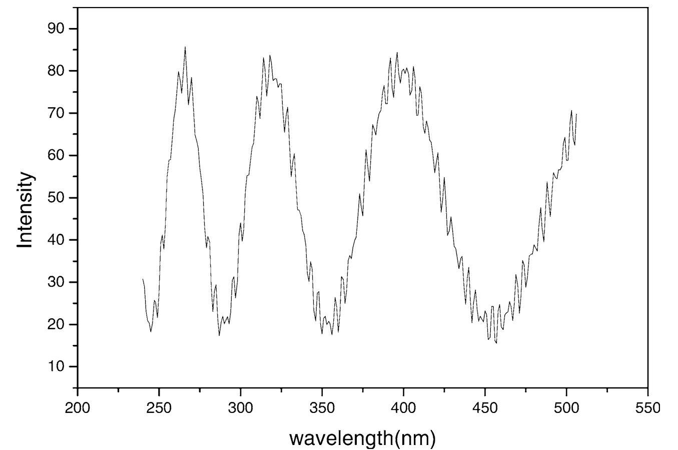

Fig. 5 Interference pattern due to vibration

This effect is represented in Fig. 5 when $\kappa_c \cdot (d/h) = 0$ and $\varepsilon_\theta = 0.1$ (random noise between 0 and 0.1), where the vibration appears to be an additive noise and easier to handle than the attenuation effect of the chemical because the chemical effect is linearly dependent on the wavelength in Eq. 8.

3 Thickness measurement of thin film

Thickness of thin film can be calculated basically using Eq. 8 by measuring the spectral intensity $\boldsymbol{I}$ of reflected light from the thin film on the wafer although the vibration level ε_θ and the chemical effect $\kappa_c d$ are unkown in general. If the extinction effect of chemical film and vibration are not small, the interference signal can be corrupted very much by the disturbances and may lead to an large error. However, in case that the attenuation of the light inside the film and the chemical is small and the vibration level is not high, the fourth and fifth terms of the interference pattern in Eq. 8 becomes small comparing with other terms. Fortunately the films and the chemical flow considered in this paper are so thin, hundreds of nanometers, that the extinction effect is very small. On these assumptions, the effects of the chemical and vibration can be treated as a noise with non-zero mean and a specific variance as can be seen from Eq. 8. If these noise-like effects are removed somehow by means of filtering technique and curve fitting, the film thickness h can be easily calculated from the filtered intensity signal $\hat{I}(v)$ in Eq. 8 by the following relations (Wang et al. 1995).

1. In case that the film thickness h is very thick comparing to the wavelength λ, i.e., $h/\lambda >> 1$ or $hv >> 1$. Multiple minimum and maximum peaks are obtained and the thickness of the film is calculated using any adjacent two ultimate peaks at υ_m and υ_{m+1} by

$$h = \frac{\pi m}{2 n_1 v_m}, \text{ where the positive integer } m = \frac{v_{m+1}}{v_{m+1} - v_m} \tag{9}$$

2. In case that the film thickness h is as thick as the wavelength λ, i.e., $h/\lambda \sim 1$ or $h\,\nu \sim 1$. Interference occurs one time. Either of minimum peak or maximum peak appears in the spectrum from which the thickness of the film is calculated by

$$h = \frac{\pi}{n_1 \upsilon_{\min}} \text{ for the min. peak,} \qquad h = \frac{\pi}{n_1 v_{\max}} \text{for the max.peak} \tag{10}$$

3. In case that the film thickness h is smaller than the wavelength λ, i.e., h/λ or hv Interference peak cannot be seen from the spectrum because the argument of the cosine function becomes very small. The thickness of the film is obtained by

$$h = \frac{1}{4\pi n_1} \sqrt{f(v)}, \text{ where } f(\upsilon) = \frac{\partial^3 I(v)}{\partial v^3} \Big/ \frac{\partial I(v)}{\partial v} \tag{11}$$

4 Experimental setup and signal processing

4.1 Configuration of interferometry system

Measurement system developed for the experiment is composed of three parts, which are a light source (Tungsten-Halogen lamp) generating a wide-band white light from UV to visible, a spectrometer (Ocean Optics S2000-UV-VIS, USA), and an optical probe detecting the reflected light from the wafer. The light signal is detected by an optical lens system placed 200 mm high above the wafer with a focusing lens for increasing the distance between the probe and the wafer without losing the reflected light power. The reason is that the probe may be damaged by the fumes produced by the chemicals and there should be an enough space to transport and handle the wafer. The optical signal measured and transferred through the optical fiber of 400 μm diameter to the spectrometer is A/D converted into 2,048 data with 2 MHz sampling rate in 20 ms as shown in Fig. 6. Thin films on 12-inch wafer specimens prepared for the thickness measurement include silicon oxide (100 nm/500 nm/600 nm in thickness) and poly-silicon (200 nm and 300 nm) fabricated and inspected very precisely in the factory. A simple proto-type of spin etcher shown in Fig. 7 is constructed to rotate the wafers and spray

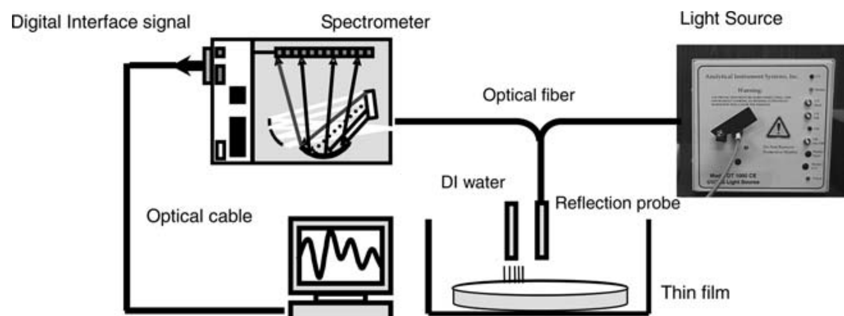

Fig. 6 Configuration of white light interferometry system

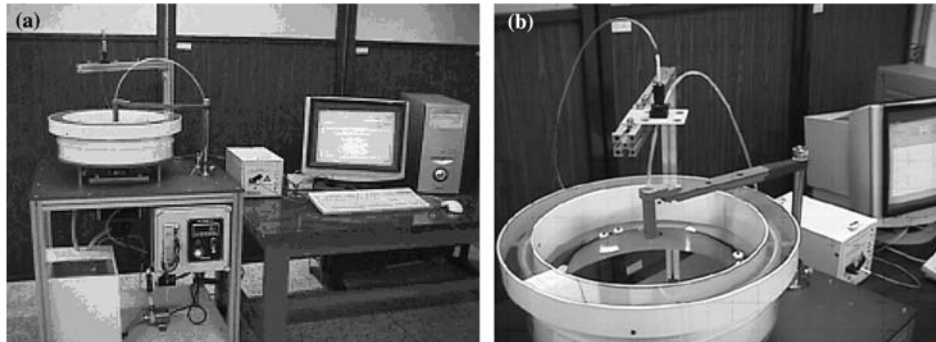

Fig. 7 Photograph of experimental setup (**a**) interferometry system (**b**) test wafer

de-ionized (DI) water instead of the hazardous chemicals for the safety reason and connected with the measurement system (EPD) developed for this study. The use of DI water instead of the chemical does not make big difference in the experimental results since chemical solutions used for etching process in semiconductor manufacturing line contain only few percentages of toxic chemicals like HF and NNO_3 in DI water. Rotating speed of the proto-type spin etcher is designed to control manually using DC-servo motor from 60 rpm to 3,600 rpm and the flow rate of DI water circulating in the closed loop by pump is also regulated.

4.2 Noise filtering using adaptive algorithm

As indicated in the Sect. 3, the interference signal $\boldsymbol{I}(v)$ contains not only the thickness information but also the disturbance signals from vibration and chemicals plus other noise sources like a statistical and electrical noise induced by light photons and measurement instruments in experiment. In order to determine the film thickness using Eqs. 9, 10 and 11 from this corrupted signal $\boldsymbol{I}(v)$, adaptive filter is adopted in this study to remove the disturbing noises of different characteristics. Let $S(\nu)$ be the degraded noisy signal of the spectrum signal $\boldsymbol{I}(v)$ by the additive noise $n(\nu)$ which includes all of the noises considered above, i.e.,

$$S(v) = \boldsymbol{I}(v) + n(v), \tag{12}$$

where $n(\nu)$ is assumed as a random signal with non-zero mean and variance σ^2. Then the optimum estimator $\hat{I}(v)$ of the signal $\boldsymbol{I}(v)$ is computed from the adaptive algorithm by (Lee 1980).

$$\hat{\boldsymbol{I}}(v) = \overline{S}(v) + g(v)[S(v) - \overline{S}(v)], \text{where the gain}$$
$$g(v) = \frac{Q(v)}{Q(v) + \sigma^2}, \tag{13}$$

where $\overline{S}(v)$ and $Q(\nu)$ are a-priori known mean and variance of $S(\nu)$ at a point ν. This adaptive filter acts like a high pass filter in a region where the variance of the signal $S(\nu)$ is large, i.e., the signal will be sharpened. Similarly, it behaves like a low-pass filter in a region where the variance of a signal is small; in this case the signal will be smoothed. Window size (frequency band or wavelength band) in this filter will greatly affect the quality of processed signal due to the local statistics in the window. If the window size is too small, the noise filtering algorithm is not effective. If the window is too large, subtle details of the signal will be lost in the filtering process. Therefore, it is necessary to optimize the effective band width for the signal from the preliminary experiments. The bandwidth of wavelength used for filtering in experiment is 20 nm for best performance.

4.3 Calculation of film thickness by curve fitting

Curve fitting is very important not only to reduce the random noise but also to determine with high accuracy the wavelength at which the maximum or minimum interference occurs in the spectrum. Even though the noise is reduced by the adaptive filtering, the wavelength of extreme peaks is difficult to find from the filtered spectrum because the spectrum near the peak points is very sensitive to the small noise which may cause an error in the film thickness. Thus it is necessary to find a smooth mathematical function that represents the measured interference pattern $\boldsymbol{I}(v)$ as precisely as possible from the corrupted noisy signal due to the vibration and the chemical flow. Polynomial function is used for this curve fitting because the derivation and root-finding for the maximum and minimum can be performed very easily and fast. Several orders of the polynomial are tested and found to be almost same in performance if it is higher than third order. Extreme points of the polynomial function, which is expressed as ν_m in Eq. 9, are calculated by finding the roots of the first derivative of the function using Newton-Rapson method. In order to do these successive procedures including the adaptive filtering and manipulation of the spectrum signal in easy manner, a Window based signal processing program written in C++ program is developed. The program controls the spectrometer, select the spectrum range of interest by the menu button on the screen, and perform the curve fitting and root finding automatically. One of the measurement results obtained by the program is shown in Fig. 8, where a noisy spectrum signal of oxide film is represented well by a fourth order polynomial function.

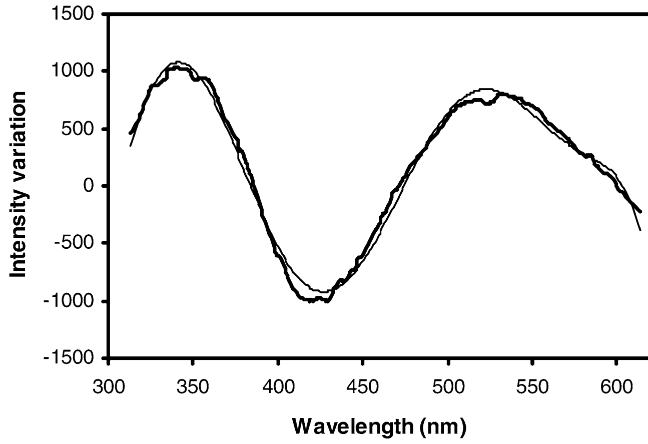

Fig. 8 Curve fitting of a noisy interference spectrum for oxide film

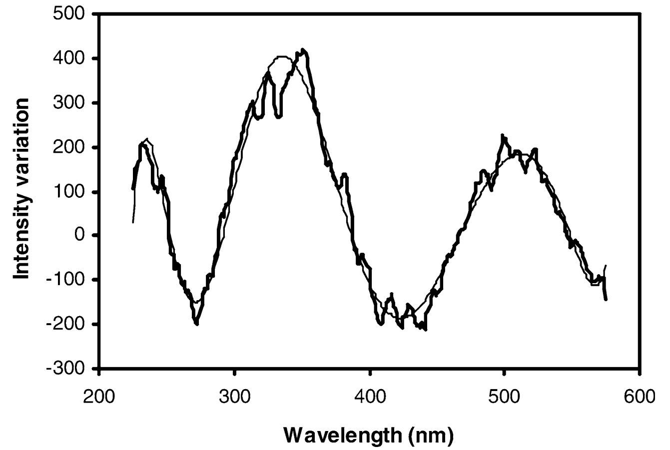

Fig. 10 Polynomial curve fitting of the interference spectrum from 600 nm oxide film

5 Experimental results and discussion

Silicon-oxide and poly-silicon films widely used in the semiconductor manufacturing processes are tested in experiment to investigate the performance and feasibility of the white light interferometry system and the signal processing program developed in this study. Thin films are deposited on the 12-inch wafer in the factory using CVD and inspected by ellipsometry. A bare wafer without any films is also prepared to obtain a reference signal from the silicon substrate. The bare wafer is mounted first on the spinner of the spin etcher as shown in Fig. 7 without spinning to measure the reflection light signal from the silicon substrate using upright reflection probe. The signal is analyzed by the spectrometer and the spectrum of the signal is stored in the computer as a reference spectrum. This reference spectrum is used later to remove the background spectrum from the room environment and the characteristic spectrum of the light source. By doing this procedure, the noise and characteristic peaks from fluorescent lights and bulbs, or even the light source in the laboratory room can be canceled out from the interference signal. Then the wafer with thin film is placed and spin on the spinner at 1,200 rpm, at which speed the vibration level is detected about 50 μm in peak-to-peak around the outer rim of the wafer. DI water is supplied on the center of the rotating wafer through a small hose above the spinner at the flowing rate of 0.3 l/min as shown in Fig. 7. The water is then spread out into a very thin film with the relatively uniform thickness. Spectrums of the reflected light from the oxide and poly-silicon films in this operating condition are measured and one example for these spectrums of 500 nm silicon-oxide film is presented in Fig. 9. In this figure the lower spectrum is the raw spectrum (non scale) acquired from the film and the upper one is the interference spectrum obtained after subtracting the raw spectrum by the reference spectrum. In Fig. 9, it can be seen that a clear sinusoidal interference pattern is observed over the spectrum mainly in the ultraviolet region. This part of the interference spectrum is selected and zoomed using the cursor in the screen or automatically by the signal processing program. Figure 10 represents this example, in which the spectrum from 600 nm oxide film is enlarged and curve fitted using a fourth-order polynomial function. Another interference

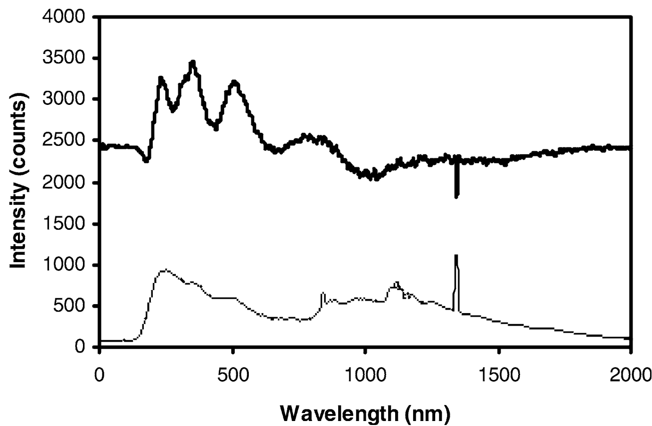

Fig. 9 Spectrum from a bare wafer and 500 nm oxide film

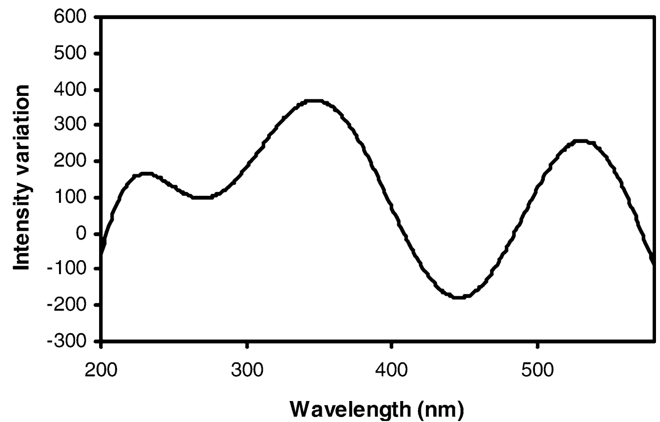

Fig. 11 Curve fitted interference spectrum for 500 nm oxide film

Table 1 Experimental results for thickness measurement

Types of thin film	Measurement results (nm)	Error (%)
Oxide 100 nm	98.2	1.8
Poly 200 nm	196.9	1.5
Poly 300 nm	302.4	0.8
Oxide 500 nm	501.2	0.2
Oxide 600 nm	600.7	0.1

spectrum produced by the program after the curve fitting is described in Fig. 11 for 500 nm oxide film. This curve is used as the intensity function $\boldsymbol{I}(v)$ of Eq. 9 through Eq. 11 to calculate the thickness of the films. Total time for the acquisition of the spectrum and signal processing for thickness measurement at a point on the wafer takes about 400 ms, which comes from mainly integration time to collect the enough intensity of the reflected light. Therefore the processing time can be reduced remarkably if more powerful light source is used.

Table 1 summarizes the experimental results for the thin films, where a very good accuracy can be seen and the maximum error of 1.8% is achieved in the presence of vibration at 1,200 rpm and the water flow on the wafer. For both of silicon oxide and poly-silicon films, more accurate result is obtained when the thickness of the film increases. This reason is that the phase difference of the reflected light in the film becomes large if the film is thick comparing with the wavelength, so that SNR increases. Errors observed in case of the oxide films thicker than 500 nm is less than 0.5% at all measuring points of the wafer. Adaptive filtering and the curve-fitting algorithm presented in the paper are proved to work well with the interferometry sysem from the experimental results. Although the vibration itself produces more noise as the spinning speed increases, the noise is removed efficiently by the adaptive filter and the curve fitting. However, the programs do not work well at a low rotating speed below 500 rpm because the attenuation effect increases very much especially in UV band as the water film becomes thick at the low speed.

6 Conclusion

Mathematical model for a single layer wafer subject to vibration and chemical flow in spin etchers is proposed and the effects of vibration and chemical fluid film on the light interferometry are described. From the model, an explicit mathematical expression for the interference pattern corrupted by vibration and chemical film are derived. Vibration affects the interference spectrum in such way as it behaves like a random noise corrupting the interference signal. The vibration-induced noise increases over the entire spectrum range as the vibration level increases with rotating speed. Chemical flow makes little effects on the spectrum data if the rotating speed is high over 500 rpm, where the film get very thin. But when the film thickness increases as the rotating speed reduces, the chemical (DI water) distorts the interference spectrum pattern severely.

A prototype real-time thickness measurement system and signal processing program for spin etcher have been also developed to measure the thin film thickness of 12-inch wafers based on the mathematical model using the wide-band white light interferometry. Adaptive filtering and curve fitting technique are applied to determine the thickness of the silicon oxide and poly-silicon films on the wafer from the interference pattern over the wide range of wavelength. From the experimental results, the wide band white light from UV to visible range is proved to be very effective to reduce the measurement error due to the vibration and the chemical flow (DI water flow) in the spin etcher. Accuracy of the measurement achieved in experiment is approximately within 1.8% of film thickness at the rotating speed of 1,200 rpm and at the flow rate of 0.3 l/min. The accuracy of measurement decreases relatively as the film thickness decreases. The reason is partly because the SNR becomes low according to the small change of phase made in the very thin film and partly because of the error produced by curve fitting and differentiation.

Acknowledgements This study was supported by University Industrial Technology Force(UNITEF) of Korea. Test wafer and evaluation of thin films are supported by Korea DNS. Each of the financial and technical support is gratefully acknowledged.

References

Kim S, Kim G (1999) Thickness-profile measurement of transparent thin-film layers by white-light scanning interferometry. Appl Opt 38(28):5968–5973

Lee JS (1980) Digital image enhancement and noise filtering by use of local statistics. IEEE Trans Pattern Anal Machine Intell PAMI 2(2):165–168

Maynard HL, Hershkowitz N (1995) Thin-film interferometry of patterned surfaces. J Vac Sci Tech B 13(3):848–857

Quirk M, Serda J (2001) Semiconductor manufacturing technology. Prentice Hall, New Jersey

Wang D, Zhang H, Yang Y, Zhang Y (1995) Ultrathin thickness and spacing measurement by interferometry and correction method. SPIE 2542:129–135

Xu Y, Li YJ (1995) Surface profile measurement of thin films using phase-shifting interferometry. SPIE 2545:238–248